# On the differential geometry of interatomic surfaces

**Paul L.A. Popelier**

**Abstract**: Using differential geometry, we propose the total curvature of interatomic surfaces to characterize bonds. In this way visual interpretations of interatomic surfaces are now rigorously quantified. The analysis of the intrinsic geometry of an interatomic surface is implemented in the program MORPHY 2.0. It is shown that the total curvature depends on anionic polarizability, electronegativity differences, and steric effects determined by the total chemical environment of the bonded atoms in question. In general the proposed index measures the external chemical distortion of an atom in a molecule. It can be used in the context of uniform electric fields and in conformational studies.

*Key words*: interatomic surfaces, differential geometry, total curvature.

**Résumé** : Utilisant la géométrie différentielle, on propose la courbature totale des surfaces interatomiques pour caractériser les liaisons. De cette façon, des interprétations visuelles des surfaces interatomiques sont maintenant rigoureusement quantifiées. L'analyse de la géométrie intrinsèque d'une surface interatomique est introduite dans le programme MORPHY 2.0. Il a été démontré que la courbature totale dépend de la polarisabilité anionique, des différences d'électronégativité et des effets stériques déterminés par l'environnement chimique total des atomes en question qui sont liés. En général, l'indice proposé mesure la distorsion chimique externe d'un atome dans une molécule. On peut l'utiliser dans le contexte de champs électriques uniformes et dans des études conformationnelles.

*Mots clés* : surfaces interatomiques, géométrie différentielle, courbature totale.

[Traduit par la rédaction]



## 1. Introduction

The gradient vector field of the charge density ρ is the carrier of the topological information hidden in molecules, complexes, and crystals. It naturally partitions these systems into atomic basins, each of which adopts a particular shape governed by the *total* charge density. In the course of the last two decades many publications in the field of "Atoms in Molecules" (AIM) have shown pictures of gradient vector fields of ρ revealing a wealth of atomic shapes.

It emerges that some shapes recur repeatedly like the signature of an atom in a given chemical environment (1). On the other hand, it also appears that the geometry of the interatomic surfaces (IAS) that bound the atomic basin is very sensitive to the full chemical environment of the atom.

In view of these observations, the introduction of a measure to quantitatively characterize the shape of an IAS would be timely. For that purpose we propose to use concepts from a mathematical branch called differential geometry since it rigorously provides intrinsic properties of geometrical objects using calculus.

First, selected differential geometrical concepts are briefly reviewed and immediately illustrated with a simple (parametrized) model surface. In Sect. 3.1 we concisely expound on how the analytical expression for an interatomic surface is constructed. Some technical details on the computation of the total curvature $C$ are given in Sect. 3.2. The last section (Sect. 4) presents various data sets of total curvatures for small molecules. The meaning of this measure is interpreted for a series of ionic lithium compounds and related to the behaviour of the IAS in a uniform electric field. Inspecting the hydride series $AH_n$, it is suggested that charge transfer influences the total curvature. It is demonstrated by means of a series of 10 methyl derivatives that $C$ does not solely parallel charge transfer. Finally, it is shown that our index can be used in conformational studies (e.g., ethane).

Received October 12, 1995.

*This paper is dedicated to Professor Richard F.W. Bader on the occasion of his 65th birthday.*

**P.L.A. Popelier.**[1] University Chemical Laboratory, Lensfield Road, Cambridge CB2 1EW, U.K.

[1] Present address: Department of Chemistry, University of Manchester Institute of Science and Technology, PO Box 88, Manchester M60 1QD, United Kingdom. Telephone: 44-161-2004511. Fax: 44-161-2367677. E-mail: pla@umist.ac.uk

## 2. Mathematical concepts

Differential geometry is the study of geometric figures using the methods of calculus. In particular, the introductory theory investigates curves and surfaces embedded in three-dimensional Euclidean space (2). It is a vast and rich area of mathematics (3–5) from which we will selectively sample and review the elements neccessary for the present investigation. Although most elegant and compact, we have chosen not to formulate the following equations along the lines of tensor analysis.

It can be proven that a curve in three-dimensional space is uniquely determined by two local invariant quantities, curvature and torsion, as functions of arc length. Similarly, a surface is uniquely determined by local invariant quantities called the first and second fundamental forms. In the following brief review, $\boldsymbol{x} = \boldsymbol{x}(u, v)$ denotes a coordinate patch on a sufficiently differentiable surface. For convenience we introduce the notation $\boldsymbol{x}_u \equiv \partial\boldsymbol{x}/\partial u$ and $\boldsymbol{x}_v \equiv \partial\boldsymbol{x}/\partial v$, such that

**Fig. 1.** Representation of two simple surfaces described by the model equation [2] (see text). The left surface corresponds to $\alpha = 1$ and $\beta = -1$ and is hyperbolic. The right surface is elliptic and has been generated with both parameters $\alpha$ and $\beta$ set to 1. The origin of each surface is marked by a black dot.

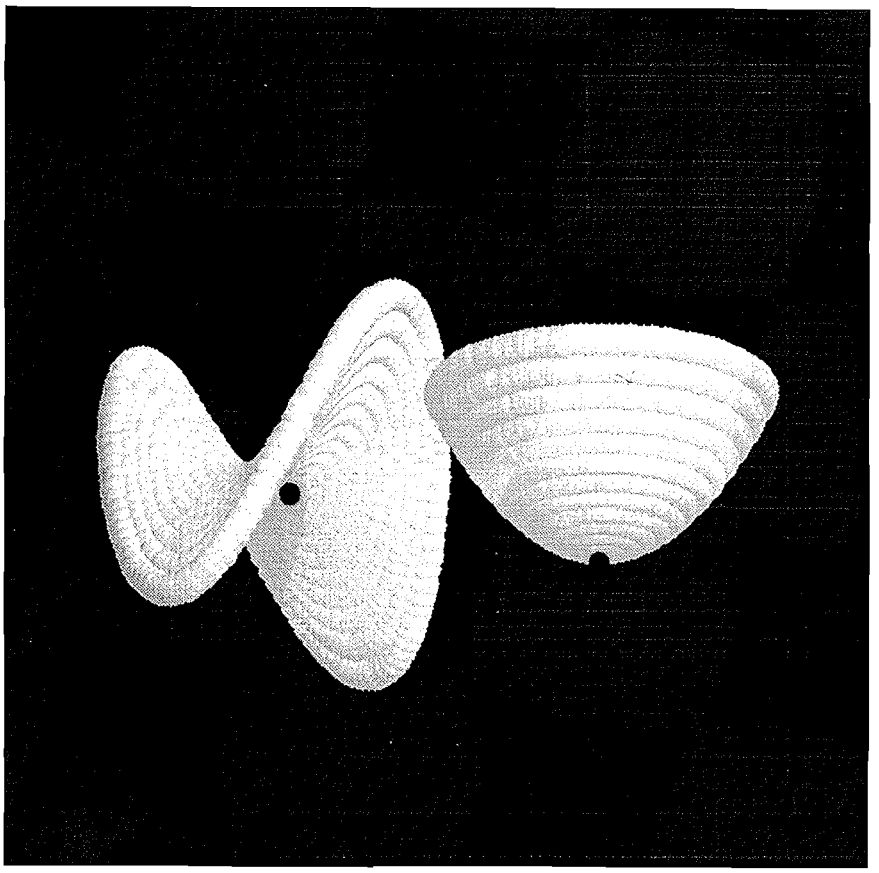

$d\boldsymbol{x} = \boldsymbol{x}_u du + \boldsymbol{x}_v dv$. The function $I_1$ defined below is called the *first fundamental form* of $\boldsymbol{x}$.

$$[1] \qquad \begin{aligned} I_1 &= (\boldsymbol{x}_u \cdot \boldsymbol{x}_u)du^2 + 2(\boldsymbol{x}_u \cdot \boldsymbol{x}_v)du dv + (\boldsymbol{x}_v \cdot \boldsymbol{x}_v)dv^2 \\ &= E du^2 + 2F du dv + G dv^2 \end{aligned}$$

where $E = \boldsymbol{x}_u \cdot \boldsymbol{x}_v$, $F = \boldsymbol{x}_u \cdot \boldsymbol{x}_v$, and $G = \boldsymbol{x}_v \cdot \boldsymbol{x}_v$. The quantities $E$, $F$, and $G$ are called the *first fundamental coefficients.*

As a direct illustration of the developed theory we will compute essential quantities defined by these and following equations for a simple model surface described by:

$$[2] \qquad \boldsymbol{x}(u, v) = u\boldsymbol{e}_1 + v\boldsymbol{e}_2 + (\alpha u^2 + \beta v^2)\boldsymbol{e}_3$$

where $\boldsymbol{e}_1$, $\boldsymbol{e}_2$, and $\boldsymbol{e}_3$ are the unit vectors of a global axis system, $u$, $v$ are the independent variables, and $\alpha$, $\beta$ are parameters introducing the appropriate flexibility to illustrate certain surface characteristics semiquantitively. Figure 1 represents two examples of simple surfaces described by eq. [2]. The left surface corresponds to $\alpha = 1$, $\beta = -1$ and the right one to $\alpha = 1$, $\beta = 1$.

Clearly, using the first derivatives

$$[3] \qquad \begin{aligned} \boldsymbol{x}_u &= \boldsymbol{e}_1 + 2\alpha u \boldsymbol{e}_3 \\ \boldsymbol{x}_v &= \boldsymbol{e}_2 + 2\beta v \boldsymbol{e}_3 \end{aligned}$$

we obtain for the first fundamental coefficients:

$$E = \boldsymbol{x}_u \cdot \boldsymbol{x}_u = 1 + 4\alpha^2 u^2$$

$$[4] \qquad F = \boldsymbol{x}_u \cdot \boldsymbol{x}_v = 4\alpha\beta uv$$

$$G = \boldsymbol{x}_v \cdot \boldsymbol{x}_v = 1 + 4\beta^2 v^2$$

The first fundamental form $I_1$ is positive definite and depends only on the surface and not on the particular representation. The first fundamental coefficients themselves are not invariant under a parameter transformation. Denoting the dimensions of $u$ and $v$ by $D_u$ and $D_v$, respectively, and knowing that components of $\boldsymbol{x}$ are expressed in units of length or $L$, it is clear that components of $\boldsymbol{x}_u$ have the dimension $L/D_u$. The dimensions of $E$, $F$, and $G$ are $L^2/D_u^2$, $L^2/D_uD_v$, $L^2/D_v^2$, respectively.

An important intermediate quantity is $EG - F^2$ and it can be proven that

$$[5] \qquad EG - F^2 = |\boldsymbol{x}_u \times \boldsymbol{x}_v|^2$$

The area $A$ of a surface patch is calculated with the aid of this quantity by the double integral:

$$[6] \qquad A = \int\int \sqrt{EG - F^2}\, du dv$$

In this work, areas of patches on interatomic surfaces approximating this integral are obtained by Gauss–Legendre quadrature. For the model surface this quantity amounts to:

$$[7] \qquad EG - F^2 = 4\alpha^2u^2 + 4\beta^2v^2 + 1$$

In an analogous manner we now proceed to define the *second fundamental form* denoted by $I_2$ by:

$$[8] \qquad \begin{aligned} I_2 &= -\mathrm{d}\boldsymbol{x}\cdot\mathrm{d}\boldsymbol{N} = -(\boldsymbol{x}_u\mathrm{d}u + \boldsymbol{x}_v\mathrm{d}v)\cdot(\boldsymbol{N}_u\mathrm{d}u + \boldsymbol{N}_v\mathrm{d}v) \\ &= L\mathrm{d}u^2 + 2M\mathrm{d}u\mathrm{d}v + N\mathrm{d}v^2 \end{aligned}$$

where $L = -\boldsymbol{x}_u\cdot\boldsymbol{N}_u$, $M = -\frac{1}{2}(\boldsymbol{x}_u\cdot\boldsymbol{N}_v + \boldsymbol{x}_v\cdot\boldsymbol{N}_u)$, $N = -\boldsymbol{x}_v\cdot\boldsymbol{N}_v$, and $\boldsymbol{N}$ is the unit normal defined by:

$$[9] \qquad \boldsymbol{N} = \frac{\boldsymbol{x}_u \times \boldsymbol{x}_v}{|\boldsymbol{x}_u \times \boldsymbol{x}_v|}$$

The functions $L$, $M$, and $N$ are called the *second fundamental coefficients*.

As before, the function $I_2$ is invariant (in the same sense that $I_1$ is invariant) under a parameter transformation that preserves the direction of $\boldsymbol{N}$.

Alternative expressions for $L$, $M$, and $N$ that we have implemented for this work are

$$[10] \qquad L = \boldsymbol{x}_{uu}\cdot\boldsymbol{N}, \qquad M = \boldsymbol{x}_{uv}\cdot\boldsymbol{N}, \qquad N = \boldsymbol{x}_{vv}\cdot\boldsymbol{N}$$

The results for these newly introduced quantities for the model surface are

$$[11] \qquad \boldsymbol{x}_{uu} = 2\alpha\boldsymbol{e}_3, \qquad \boldsymbol{x}_{uv} = 0, \qquad \boldsymbol{x}_{vv} = 2\beta\boldsymbol{e}_3$$

$$[12] \qquad \boldsymbol{x}_u \times \boldsymbol{x}_v = 2\alpha u\boldsymbol{e}_1 - 2\beta v\boldsymbol{e}_2 + \boldsymbol{e}_3$$

$$[13] \qquad |\boldsymbol{x}_u \times \boldsymbol{x}_v| = (4\alpha^2u^2 + 4\beta^2v^2 + 1)^{-1/2}$$

$$[14] \qquad L = \boldsymbol{x}_{uu}\cdot\boldsymbol{N} = 2\alpha(4\alpha^2u^2 + 4\beta^2v^2 + 1)^{-1/2}$$

$$M = \boldsymbol{x}_{uv}\cdot\boldsymbol{N} = 0$$

$$N = \boldsymbol{x}_{vv}\cdot\boldsymbol{N} = 2\beta(4\alpha^2u^2 + 4\beta^2v^2 + 1)^{-1/2}$$

Since $\boldsymbol{N}$ is dimensionless the dimension of $L$ is $L/D_u^2$.

A discriminant $D$ defined as $LN - M^2$ determines qualitatively the nature of the surface in the neighbourhood of a point. We can distinguish four cases: a point is elliptic, hyperbolic, parabolic, or planar when $D$ is strictly positive, strictly negative, zero (without $L$, $M$, $N$ all being zero), and when $L = M = N = 0$, respectively. It should be pointed out that ellipticity, etc. is a *local* property, i.e., it refers to the character of a single point on a surface, not to the global surface. This classification is again independent of the representation of the surface. The discriminant for our model surface is given by:

$$[15] \qquad LN - M^2 = 4\alpha\beta(4\alpha^2u^2 + 4\beta^2v^2 + 1)^{-1}$$

In the neighbourhood of an elliptic point the surface lies on the same side of the tangent plane at the point. On the other hand, the surface lies on both sides of the tangent plane in the neighbourhood of a hyperbolic point. Such a point is easy to visualize as the center of an ordinary saddle.

The central quantity for our present discussion is the *Gaussian curvature* $K$ at a given point. A convenient definition is

$$[16] \qquad K = \frac{LN - M^2}{EG - F^2}$$

This is again an invariant property of the surface. Since $(EG - F^2) > 0$ the sign of $K$ classifies a point as elliptic, hyperbolic, or parabolic (or planar). It is clear that on each point of a plane the Gaussian curvature $K$ vanishes. Another useful special case is the spherical surface. For every point on a sphere with radius $a$ we have $K = 1/a^2$. It follows from the previous dimensional analysis that the dimension of $K$ for a point on a general surface is indeed $1/L^2$. The Gaussian curvature for the model surface is

$$[17] \qquad K = 4\alpha\beta(4\alpha^2u^2 + 4\alpha^2v^2 + 1)^{-2}$$

As an example we focus on the origin of each surface in Fig. 1. These points are marked by black dots and correspond to $u = v = 0$. Consequently, $K = 4\alpha\beta$ and the classification of the origin depends only on the signs of $\alpha$ and $\beta$ and on whether they vanish. It then follows that the origin in the left surface is hyperbolic and in the right surface is elliptic. Since the denominator of $K$ and $(4a^2u^2 + 4a^2v^2 + 1)^{-2}$ in eq. [17] is strictly positive, this statement is true for any point on the respective surface, not just the origin. Furthermore, increased values of $\alpha$ or $\beta$ steepen the surface at the origin and increase the Gaussian curvature, which is in line with geometrical intuition.

When the Gaussian curvature is integrated over a surface $S$ we obtain the *total curvature* $C$.

$$[18] \qquad C = \int\int_S K\mathrm{d}S$$

It is very important to note that $C$ is dimensionless. It adopts the following analytical form for the model surface.

$$[19] \qquad \begin{aligned} C &= \int\int_R K\mathrm{d}S = \int\int_D K(\boldsymbol{x}(u, v))|\boldsymbol{x}_u \times \boldsymbol{x}_v|\mathrm{d}u\mathrm{d}v \\ &= 4\alpha\beta\int_0^u\int_0^v (4\alpha^2u^2 + 4\alpha^2v^2 + 1)^{-3/2}\mathrm{d}u\mathrm{d}v \end{aligned}$$

If interatomic surfaces were *compact*, characterizing them using the total curvature $C$ would not quite lead to a useful classification. This statement is a corollary of two well-known theorems, as is explained below. According to the Heine–Borel theorem, a surface is compact if and only if it is bounded and closed. A sphere and a torus are examples of compact surfaces. On the other hand, the Gauss–Bonet theorem proves that for compact surfaces (which must be orientable and sufficiently differentiable) the total curvature is just a multiple of $\pi$ and is a topological invariant. The total curvature of a sphere, for example, is $4\pi$ and for a torus is zero. Since interatomic surfaces are not bounded, they are not compact. Therefore the Gauss–Bonet theorem does not apply to them. As a result we do not *necessarily* recover trivial multiples of $\pi$ when computing $C$ for an IAS.

## 3. Implementation

### 3.1 Analytical expression of the surface

An IAS consists of a bundle of gradient paths that originate at infinity and terminate at the so-called *bond critical point* (6). This point is one of the four possible types of critical points (i.e., $\nabla\rho = \mathbf{0}$) and is denoted by $(3,-1)$. It can be regarded as the center of the IAS. Gradient paths are traced by solving the following system of ordinary differential equations given an initial point through which the path is passing:

$$[20] \qquad \frac{d\boldsymbol{r}}{dl} = \frac{\nabla\rho(\boldsymbol{r})}{\|\nabla\rho(\boldsymbol{r})\|}$$

It has been shown before that solving this system with analytical tools is possible but unsatisfactory (7). A more successful scheme solves the ordinary differential equations using a numerical integrator with adaptive step-size control like the Cash–Karp–Runge–Kutta method (8) and then fits Chebyshev polynomials and trigonometric functions to the points on the IAS. Each component $x_i(l,\theta)$ of a point on the surface is then given by the *explicit* parametric equation:

$$[21] \qquad x_i(l,\theta) = \sum_{m,n}^{M,N} (d_{inm}\cos(m\theta) + d'_{inm}\sin(m\theta))T_n(l)$$

where $d_{inm}, d'_{inm}$ are fitted, $T_n$ is the $n$th degree Chebyshev polynomial, $l$ is the length of a gradient path on the IAS, and $\theta$ is an angular coordinate.

The IAS is constructed by following the gradient paths backwards, away from the bond critical point, starting from a set of *initial points*. These initial points form a circle with a small radius $r_\varepsilon$ (typically 0.001 atomic units) in the *eigenplane* (7). The Chebyshev fit only extends over the interval $[-l_{max}, 0]$.

The analytical description of the IAS leaves a small puncture near the bond critical point that we have minimalized by setting $r_\varepsilon$ to a really small value like $10^{-6}$. So, practically, we assume that the IAS is only bounded for large negative $l$ values and not for $l = 0$.

Excellent fits can be obtained with a moderate number of fitting basis functions (fewer than 50). The quality of the fit is measured by quasi-continuous error estimates such as a global root-mean-square value (7). A value of $10^{-4}$ atomic units (au) or less is quite typical for a surface up to the $10^{-9}$ au charge density contour surface. This basically means that the analytical expressions perfectly reproduce the numerical surface.

### 3.2 Calculation of total curvature

Since the availability of an analytical expression for the IAS (7) it has been possible to obtain fast and accurate surface-related derivatives for computing local and integrated surface curvatures. Derivatives of high-order Chebyshev polynomials do not pose problems and are evaluated rapidly.

It is crucial to test the stability of the total curvature $C$ with respect to various parameters. All surfaces have been fitted with Chebyshev polynomials up to order 40 and with a set of 51 trigonometric functions.[2] The relative accuracy of the differential equation integrator was kept at $10^{-4}$ (for a precise definition see ref. 8, p. 711) and the minimum allowed step size was fixed at $10^{-7}$ au.

Secondly, the behaviour of $C$ was monitored as a function of the size of the patch on the IAS. In general, interatomic surfaces extend to infinity and a well-behaved total curvature should converge with more negative $l$ values. Tests for the N|H IAS in ammonia show rather slow convergence but stability is essentially reached for $l < -10$ au (the changes in $C$ are of the order of $10^{-4}$). The total curvature varies slightly more for the C|O surface in carbon monoxide. It is well known that Gaussian functions do not properly describe the outer regions of a molecule. We must therefore suspect that gradient paths are not very meaningul in zones where the charge density is as low as $10^{-12}$ au or less, especially at a moderate level of theory like HF/6-31G**. Consequently the local curvature of the IAS in the outer region is not trustworthy. Since the total curvature is a purely geometrical quantity, not weighted by (extremely low) charge densities or their gradient, the outer region will unduly affect $C$.

This phenomenon has prompted us to compute the total curvature only for a well-defined and reliable patch on the IAS. There is good evidence that the 0.001 au charge density envelope may be considered as the practical edge of the molecule and thus of its constituent atoms. We have fitted a very accurate continuous contour line to points on the IAS where $\rho = 0.001$ au. This smooth and analytical contour line then bounds the IAS everywhere. All total curvature values quoted below have been computed with a grid extending only to the 0.001 au charge density contour level. We believe that results drawn from these numbers genuinely reflect what happens well inside the molecule and should therefore relate to chemical insight.

Finally, the effect of stability of $C$ on the quadrature grid size was explored. Throughout, we use a grid with 60 radial and 120 angular points, which is sufficient.

## 4. Applications

Before interpreting the data a general comment is worth inserting. The "outer" shape of an atomic basin is determined by the geometry of the interatomic surfaces bounding it. This is the shape we focus on in the following discussion. But an atom also has an "inner" shape, which is determined by the pattern of the gradient vector field inside the atom. One might say that gradient paths distort space. They establish non-Euclidean geodesics and exhibit a Riemannian curvature that characterizes the whole atomic subspace. This is of course the ultimate curvature to be investigated and is therefore the subject of future work.

All wave functions were generated using the program CADPAC (9) using the 6-31G** basis set (10), 6-31GE,[3] and a [13*s*5*p*/4*s*3*p*] set (4) for lithium.

Table 1 presents the total curvature for a set of four ionic closed-shell lithium compounds: LiF, LiH, $LiCH_3$, and $LiO^-$. Three quantities consistently indicate that these compounds are ionic. The charge density at the bond critical point or $\rho_b$

[2] The trigonometric basis set is $\{1, \cos(n\theta), \sin(n\theta)\}$, where $n = 1,2,\ldots,25$.

[3] The basis set is obtained from the 6-31G basis set by adding diffuse functions and polarization functions. More details are found in the CADPAC manual.

**Table 1.** The total curvature $C$ and additional quantities[a] of some ionic lithium compounds computed using two different basis sets.

| Molecule | $d$(Li–A)[b] | $\rho_b$ | $\nabla^2\rho_b$ | $q$(Li) | $L(\Omega)$ | $C$ |
|---|---|---|---|---|---|---|
| **HF/6-31G**** | | | | | | |
| LiF | 1.537 | 0.086 | 0.767 | 0.910 | $3 \times 10^{-4}$ | 1.27 |
| LiH | 1.616 | 0.036 | 0.137 | 0.898 | $7 \times 10^{-5}$ | 2.75 |
| $LiCH_3$ | 2.053 | 0.043 | 0.189 | 0.907 | $5 \times 10^{-5}$ | 3.05 |
| $LiO^-$ | 1.600 | 0.094 | 0.786 | 0.779 | $3 \times 10^{-4}$ | 2.97 |
| **HF/6-31GE** | | | | | | |
| LiF | 1.570 | 0.077 | 0.671 | 0.935 | $3 \times 10^{-4}$ | 1.49 |
| LiH | 1.622 | 0.038 | 0.138 | 0.908 | $7 \times 10^{-5}$ | 2.70 |
| $LiCH_3$ | 1.997 | 0.044 | 0.186 | 0.911 | $9 \times 10^{-5}$ | 2.95 |
| $LiO^-$ | 1.575 | 0.086 | 0.699 | 0.850 | $1 \times 10^{-4}$ | 3.92 |
| **MP2/6-31GE** | | | | | | |
| LiF | 1.593 | 0.073 | 0.596 | 0.925 | $1 \times 10^{-5}$ | 1.68 |
| LiH | 1.612 | 0.038 | 0.141 | 0.904 | $6 \times 10^{-6}$ | 2.64 |
| $LiCH_3$ | 1.994 | 0.041 | 0.181 | 0.905 | $3 \times 10^{-4}$ | 3.02 |
| $LiO^-$ | 1.678 | 0.062 | 0.472 | 0.831 | $3 \times 10^{-5}$ | 6.18 |

[a]All quantities are given in atomic units unless stated otherwise. Symbols are explained in the main text.
[b]The distance between the two nuclei is given in Å.

**Table 2.** The influence of a uniform electric field on the total curvature $C$ of the interatomic surface in the hydrogen molecule and hydrogen fluoride.

| Field[a] | $C(H_2)$ | $C$(HF) |
|---|---|---|
| −0.050 | 0.146 | 1.067 |
| −0.010 | 0.006 | 1.386 |
| −0.005 | 0.001 | 1.425 |
| −0.001 | 0.000 | 1.455 |
| 0.000 | 0.000 | 1.463 |
| 0.001 | 0.000 | 1.471 |
| 0.005 | 0.001 | 1.501 |
| 0.010 | 0.006 | 1.539 |
| 0.050 | 0.146 | 1.837 |

[a]The field strength is expressed in au.

is about 10 times smaller than for a typical covalent bond. The Laplacian at the bond critical point or $\nabla^2\rho_b$ is positive and the net charge $q$(Li) is approaching the value of exactly one. This net charge is obtained by integrating the charge density over the atomic basin of lithium and substracting this population from the nuclear charge. The integration error is typically assessed by $L(\Omega)$, which should ideally vanish (12).

It is a good approximation to regard the charge transfer from lithium to the neighbouring atom as constant within the present series since the maximum discrepancy for $q$(Li) is only 0.085 e using the 6-31GE basis set. This fact is consistent with the earlier observation of Bader and Beddall (13) for wave functions close to the Hartree–Fock limit. As expected, the well-known AIM quantities are quite insensitive to the variation in basis set. This is also true for the total curvature, with the exception of $LiO^-$ where the highly polarizable $O^{2-}$ anion benefits from the better description provided by the extra diffuse functions.

The inclusion of correlation at the MP2 level does not alter the order $LiF < LiH < LiCH_3 < LiO^-$ as ranked by the total curvature $C$. It is well known that anions are the most affected by correlation, which is reflected by the pronounced changes for $LiO^-$. It can be seen from Table 1 that all properties $d$(Li—A), $\rho_b$, $\nabla^2\rho_b$, and $q$(Li) vary considerably for this molecule and only marginally for the other molecules in this set. Since the qualitative conclusions of the present study do not alter with electron correlation we will not systematically investigate its effect on the non-ionic compounds discussed below.

Since the present molecules are nearly completely ionic one may view them as a point charge perturbing a polarizable anion. Exact calculations for the polarizability of free anions yield 15.1 au for $F^-$ (14), 206 au for $H^-$ (15), and an infinite value for $O^{2-}$ (16).[4] This is exactly the order reflected by the total curvature computed with the 6-31GE basis set, predicting that the $CH_3^-$ group must be a very polarizable charge cloud. This conclusion is plausible since the basic methyl anion has a diffuse lone pair of strong $sp^3$ character and because carbon and hydrogen have a virtually identical electronegativity.

Further evidence that the total curvature $C$ is indeed affected by the extent of polarization of an atom emerges from the behaviour of $H_2$ and HF in a uniform electric field. The results are shown in Table 2 for a field strength $E_z$ along the molecular axis varying from −0.05 to +0.05 au. Hydrogen fluoride shows an excellent linear correlation ($\rho = 0.9997$) between $C$ and $E_z$, yielding $C = 7.6973\,E_z + 1.4604$. The linear dependence for $H_2$ is weaker ($\rho = 0.9883$) and here $C = 3.0349\,E_z - 0.0094$. It is tempting to relate the slope of these equations with $\alpha_s(\Omega)$, which was previously introduced (18) as the associated contribution to the polarizability resulting from the shift in interatomic surface. Using the values quoted in ref. 18 for HF and $H_2$, the difference in response of the IAS to the applied field could be explained semi-quantitatively. The main point, however, of this small excursion is to indicate that $C$ can be used in studying atoms in electric fields and that the polarization of a charge cloud within an atomic basin does change the intrinsic geometry of its bounding IAS.

The next series of molecules constitutes the classic set of hydrides $AH_n$ where A = H, Li, Be, B, C, N, O, F and $n$ varies, producing $H_2$, LiH, $BeH_2$, $BH_3$, methane, ammonia, water and hydrogen fluoride. Detailed three-dimensional pictures of the atoms encompassed by this set have recently been published for the first time (1). Figure 2 shows the C|H IAS in methane and the corresponding contour map for the Gaussian curvature $K$.

From Table 3 it is seen that the total curvature for the A|H IAS increases steadily as the charge transfer from H to A increases. Since it was shown before that the charge transfer defined by AIM recovers the basic idea underlying electronegativity, it seems plausible to surmise that the total curvature increases with increasing electronegativity.

[4] The species $O^{2-}$ is unstable with respect to decomposition into a free $O^-$ ion and a free electron; see ref. 17.

(a)

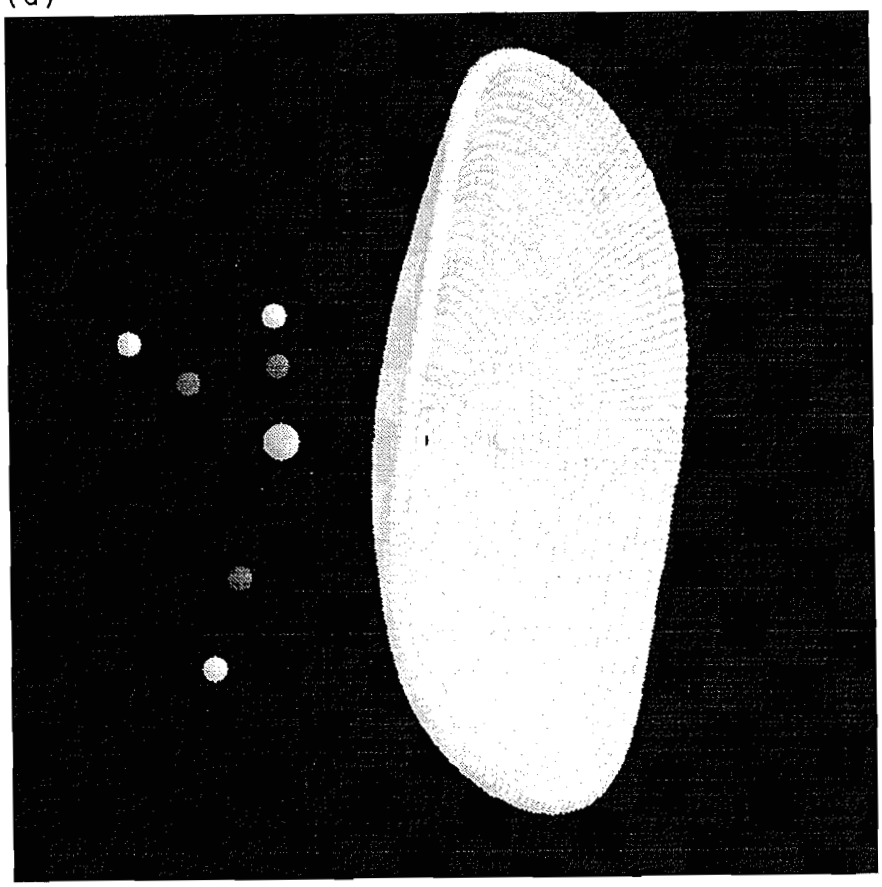

(b)

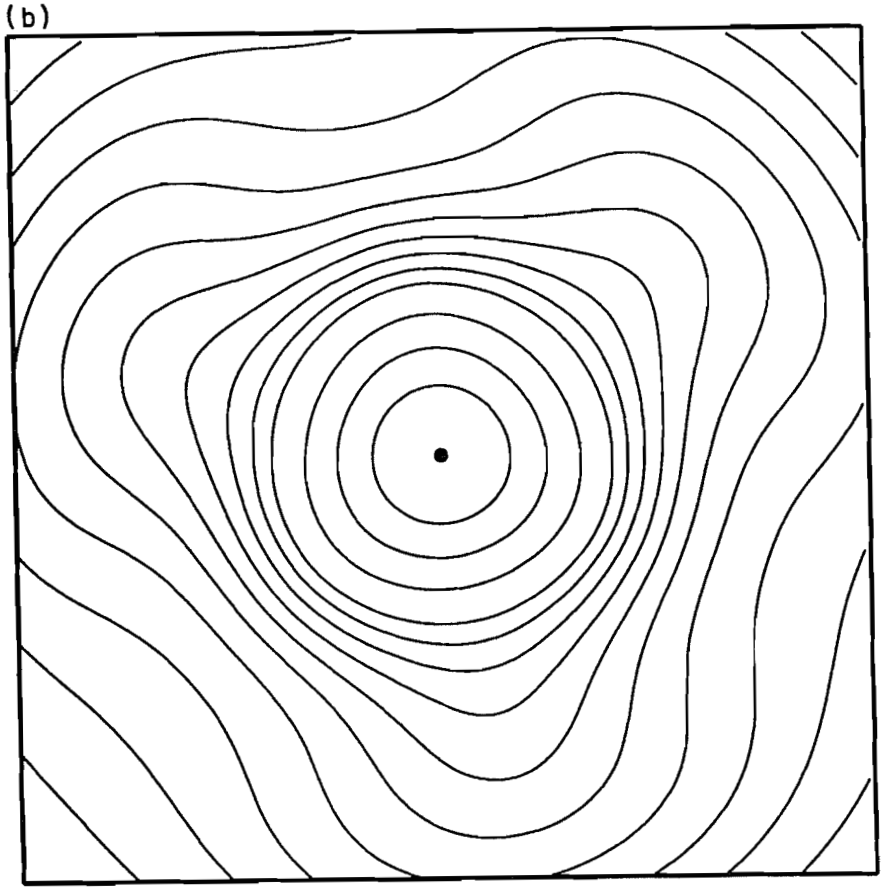

**Fig. 2.** (*a*) A three-dimensional representation of the C|H interatomic surface in methane. The bond critical points are marked by grey dots. This picture should be compared with the corresponding contour map of Fig. 2*b*. (*b*) A contour map of the Gaussian curvature $K$ of the interatomic surface between C and H in methane. The outer contour line corresponds to a curvature of 0.001 and the contours increase as 0.005, 0.01, 0.015, 0.02, 0.025, 0.03, 0.035, 0.04, 0.045, 0.05, 0.06, 0.07, 0.08, and 0.09. The bond critical point is marked by a dot. Note that the expected threefold symmetry becomes more pronounced towards the outer regions of the interatomic surfaces, which correspond to an $l$ value of about −3.

**Table 3.** The charge transfer $q$ and the total curvature $C$ and area[a] for the A|H interatomic surface in the second row hydrides $AH_n$.

| Molecules | $q$(H) | $C$ | Area |
|---|---|---|---|
| $H_2$ | 0.000 | 0.000 | 28.08 |
| LiH | −0.893 | 2.741 | 28.90 |
| $BeH_2$ | −0.873 | 0.002 | 35.31 |
| $BH_3$ | −0.718 | —[b] | — |
| $CH_4$ | 0.062 | 0.692 | 32.00 |
| $NH_3$ | +0.373 | 1.084 | 24.88 |
| $OH_2$ | +0.619 | 1.297 | 19.18 |
| HF | +0.757 | 1.463 | 14.73 |

[a]The interatomic surface is bounded by a contour line of constant charge density (0.001 au). The area is given in $(au)^2$.
[b]Instabilities in the IAS prevent the computation of a reliable number at present.

Even if charge transfer does influence the total curvature,[5] it cannot be the only effect because the CH bond in methane shows virtually no charge transfer, yet the curvature amounts to 0.692. Similarly, in the $^2\Pi$ diatomic CH the total curvature is reasonable but charge transfer is essentially absent. The series of diatomics, CH, NH, OH, and HF, shows an increase in IAS total curvature resembling that of the present hydride series. These four diatomic molecules are examples of shared interactions characterized by a reasonably large value for $\rho_b$ and a (strongly) negative $\nabla^2\rho_b$ value. In NH, OH, and HF there is an increasing polarization of the shared charge towards the non-hydrogen atom, but the "mechanism" by which this might change the curvature is not clear, the more so because the bond critical point shifts as well in this series.

Because of the symmetry in methane we cannot invoke the fairly large intra-atomic dipole moment of carbon. This measure is the first moment $\boldsymbol{M}(\Omega)$ and determines the displacement of the atom's centroid of negative charge from the position of its nucleus. These contributions will cancel each other in methane and can therefore not be the cause for the shape of the C|H surface.

To shed more light on this matter we have computed the total curvature for several other C—H bonds in saturated hydrocarbons, all of which show negligible charge transfer. In staggered ethane $C = 0.996$ for all six C—H bonds, whereas in the *anti–anti* conformation of propane three types of C—H are found: $C = 1.476$ for hydrogens attached to the central methylene carbon, $C = 1.365$ or $C = 1.022$ for hydrogens attached to a methyl carbon.

It emerges from these observations that the total curvature of C|H interatomic surfaces is very sensitive to the total chemical environment. This becomes intuitively obvious on inspecting Fig. 3. As a rule, a higher number of carbons attached to the carbon of the C|H IAS will increase the total curvature. This measure seems to probe how far atoms that are "pushed" together in a molecule distort each other. "Clashes" with third-party atoms can severely modify the curvature of the IAS between two atoms. This effect has been sufficiently documented in preliminary tests in more "crowded" systems like acetamide and urea. The total curvature for the C|O IAS takes the values −0.116, 0.000, 0.022, 0.174, and 0.242 in formaldehyde, carbon monoxide, formamide, urea, and acetamide, respectively. It can visually be verified that basins that are more distorted at their boundary yield higher total curvature values for their interatomic surface(s). There is no straightforward means of reducing this emerging phenomenon to known physical principles or quantities. The question why the C|H IAS in methane has a considerable curvature is equivalent to asking why this surface simply appears the way it does. One might explain its shape as a compromise between four equally distortable hydrogen atoms covalently bound to a carbon atom with a different distortability.

It is remarkable that the total curvature of the IAS in $BeH_2$ is almost zero. The shape of this surface is quite similar to the IAS in C≡O, which also has a vanishing total curvature. This is caused by an annihilation of negative contributions to the Gaussian curvature $K$ by positive ones, as shown in Fig. 4.

This similarity can be explained by a common physical ground. Both bonds show a considerable charge transfer, the value for C≡O being 1.33 e. Given that in these molecules there is no "steric" phenomenon influencing the total curvature $C$ and assuming that charge transfer enhances $C$, we are left with the question why $C$ is nevertheless essentially zero. Carbon monoxide has a large and diffuse (weakly bound) charge distribution on carbon, which leads to a very pronounced polarization opposing the charge transfer moment. This explains the near-zero dipole moment of this molecule. Similarly, berylium has a diffuse valence density, again leading to large atomic polarization. One may hypothesize that the total curvature absorbs both the charge transfer and back-polarization effect.

The fact that the total curvature $C$ is not just mirroring charge transfer is demonstrated by a set of methyl derivatives given in Table 4. In their work on substituent effects of methyl derivatives (19), Wiberg and Breneman have ordered 20 moieties with $C_{3v}$ symmetry according to increasing pop-

[5] Ideally, one wishes to isolate the possible effect of charge transfer on the total curvature $C$. Constructing a molecule in which two of its atoms show only charge transfer without mutual polarization is virtually impossible unless one resorts to very artificial systems like $LiBe^{5+}$. This species is supposed to eliminate any polarization effect on the IAS and isolate the influence of charge transfer (if present at all) on the total curvature.

**Fig. 3.** A three-dimensional representation of three C|H interatomic surfaces in the *anti–anti* conformation of propane. The top surface has the highest total curvature ($C$ = 1.476) followed by the bottom (right) one ($C$ = 1.365). The left surface has a much lower total curvature ($C$ = 0.996), identical to the value in the staggered conformation of ethane. This picture provides visual support for the observation that $C$ is very sensitive to the total chemical environment of the atomic basin.

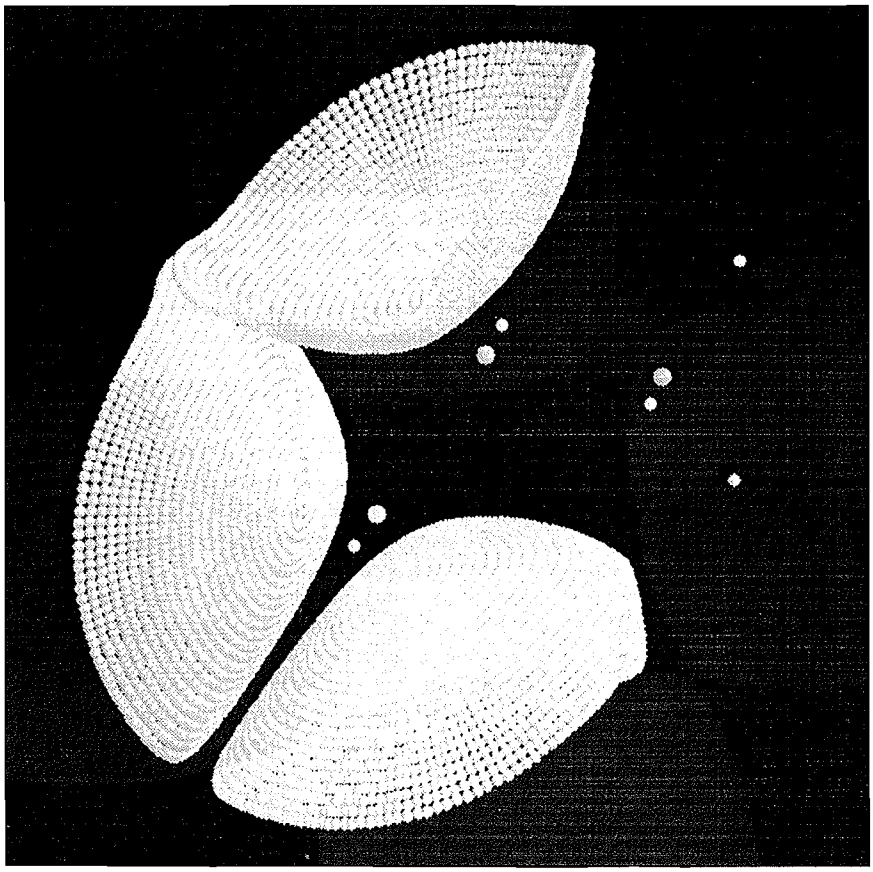



**Fig. 4.** A relief map of the Gaussian curvature $K$ of the C|O interatomic surface in carbon monoxide. In the outer region of the IAS the curvature practically vanishes, which is the equivalent of near planarity.

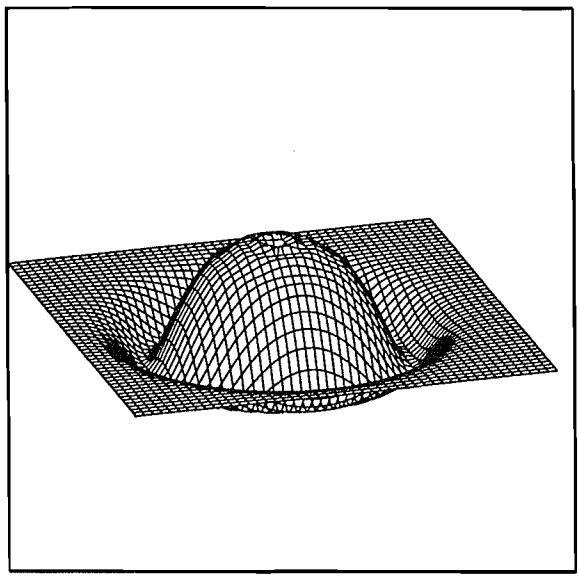

**Table 4.** The charge transfer $q$ and the total curvature $C$ and area[a] of the C|A[b] interatomic surface in methyl substituted derivatives.

| Molecules | $C$ | $q(CH_3)$[c] | Area |
|---|---|---|---|
| $CH_3Cl$ | −0.08 | +0.316 | 42.6 |
| $CH_3S^-$ | −0.08 | −0.287 | 49.3 |
| $CH_3$ C≡CH | −0.08 | +0.362 | 40.5 |
| $CH_3BeH$ | 0.00 | −0.875 | 36.5 |
| $CH_3$ C≡N | 0.03 | +0.362 | 39.4 |
| $CH_3N_2^+$ | 0.03 | +0.840 | 36.5 |
| $CH_3OLi$ | 0.12 | +0.618 | 38.9 |
| $CH_3O^-$ | 0.19 | +0.474 | 39.9 |
| $CH_4$ | 0.69 | +0.061 | 32.0 |
| $CH_3Li$ | 3.05 | −0.902 | 26.4 |

[a]The interatomic surface is bounded by a contour line of constant charge density (0.001 au). The area is given in $(au)^2$.
[b]The letter "A" represents the atom of the substituent group directly attached to the methyl carbon.
[c]The charge transfer is measured with respect to the population of the whole methyl group, which is 9.000 e. The present values are quoted from ref. 19.

**Table 5.** The total curvature $C$ and area[a] for the C—C interatomic surface in various conformations of ethane.[b]

| $\tau$[c] | $\Delta E$[d] | $C$ | Area |
|---|---|---|---|
| 0 | 12.6 | 0.000 | 42.3 |
| 15 | 10.8 | −0.054 | 42.5 |
| 30 | 6.4 | −0.168 | 42.9 |
| 45 | 1.9 | −0.267 | 43.4 |
| 60 | 0.0 | −0.304 | 43.6 |

[a]The interatomic surface is bounded by a contour line of constant charge density (0.001 au). The area is given in $(au)^2$.
[b]Ethane has been fully optimized at the 6-31G** level only fixing the torsion angles.
[c]This HCCH torsion angle is given in degrees: 0° and 60° correspond to the eclipsed and staggered conformations, respectively.
[d]This energy difference is given in kJ/mol.

ulation of the methyl group. We focus on the IAS between the methyl carbon and the substituent atom attached to it. The 10 molecules we selected from this list fall, broadly speaking, in three categories according to $C$. The first group has a very small $C$ value with the ionic compound $CH_3BeH$ again showing a vanishing total curvature. Although the population of the methyl group varies considerably in this subset, $C$ is not able to discriminate these systems very well. Under the hypothesis that the total curvature is influenced by charge transfer, polarization, and steric crowding one may speculate that these molecules have enough flexibility to allow these effects to cancel each other and reach an "atomic distortion equilibrium." The two other groups $CH_4$ and $CH_3Li$, which have been discussed before, contain only one member.

Finally, we simply point out that the total curvature index can also be applied in conformational analyses. A simple example is reported in Table 5 where the central torsion angle in ethane is varied from 0° to 60°. The total curvature of the C|C surface becomes more negative in a sinusoidal manner on going from the eclipsed to the staggered conformation. The latter IAS is represented in Fig. 5 as an example of a predominantly hyperbolic surface, because for the total curvature (which is an integral) to be negative there must be dominant contributions of surface points with a negative Gaussian curvature.

## 5. Conclusion

A purely geometrical index is proposed to characterize interatomic surfaces in molecules. This index is called the total curvature $C$ and stems from a rigorous application of differential geometry. It is dimensionless and gauges the intrinsic geometry of a surface regardless of its representation or position in space.

**Fig. 5.** A three-dimensional representation of the C|C interatomic surface in the staggered conformation of ethane. This surface has a negative total curvature.

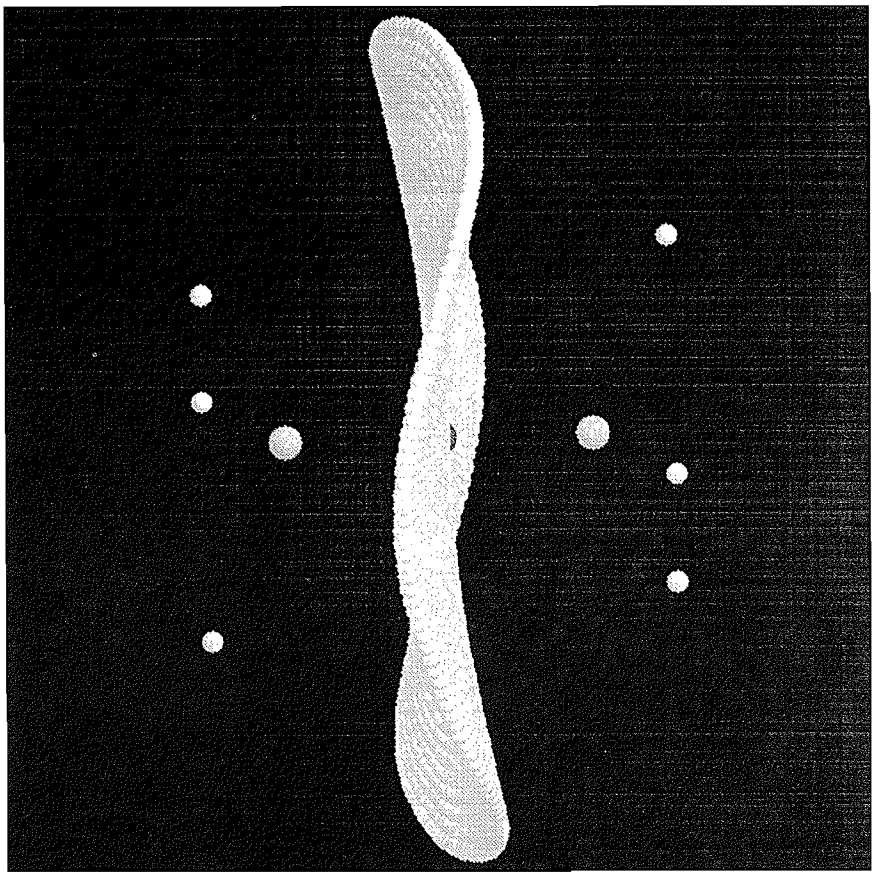

The total curvature measures the chemical distortion of an atom in a molecule, which is a combination of polarization deformation, charge transfer, and steric effects. Although it is a single-bond oriented quantity it is sensitive to the complete chemical environment of the bonded atoms.

For a series of ionic diatomics with a practically constant charge transfer, $C$ measures the distortion of the anion by the positive neighbouring charge. It is conjectured that increasing electronegativity differences between two bonded atoms increases the total curvature of the IAS. Other simultaneous influences on $C$ should be included since the charge transfer in methyl derivatives is not reflected on a one-to-one basis in the total curvature of the IAS between the methyl carbon and the substituent.

The proposed index can be used to probe the response of an IAS in uniform electric fields and can be employed in conformational studies.

It remains speculative whether a straightforward and interesting relationship exists between the HSAB principle (20) and the total curvature.

## References


1. R.F.W. Bader, P.L.A. Popelier, and T.A. Keith. Angew. Chem. Int. Ed. Engl. **33**, 620 (1994).
2. M.M. Lipshutz. Differential geometry, Schaum's outline series. McGraw–Hill, New York. 1969.
3. D.J. Struik. Differential geometry. Addison–Wesley, London. 1961.
4. V.I. Arnold. Mathematical methods of classical mechanics. 2nd ed. Springer, New York. 1989.
5. M.P. do Carmo. Differential geometry of curves and surfaces. Prentice-Hall, New Jersey. 1976.
6. R.F.W. Bader. Atoms in molecules. A quantum theory. Clarendon. Oxford. 1990.
7. P.L.A. Popelier. Theor. Chim. Acta, **87**, 465 (1994).
8. W.H. Press, B.P. Flannery, S.A. Teukolsky, and W.T. Vetterling. Numerical recipes. 2nd ed. Cambridge Press, U.K. 1992.
9. CADPAC5: The Cambridge Analytic Derivatives Package Issue 5, Cambridge, 1992. A suite of quantum chemistry programs developed by R.D. Amos with contributions from I.L. Alberts, J.S. Andrews, S.M. Colwell, N.C. Handy, D. Jayatilaka, P.J. Knowles, R. Kobayashi, N. Koga, K.E. Laidig, P.E. Maslen, C.W. Murray, J.E. Rice, J. Sanz, E.D. Simandiras, A.J. Stone, and M.D. Su.
10. R. Krishnan, J.S. Binkley. R. Seeger, and J.A. Pople. J. Chem. Phys. **72**, 650 (1980).
11. F.B. van Duijneveldt. IBM Research Report. RJ 945. 1971.
12. F.W. Biegler-König, R.F.W. Bader, and T.-H. Tang. Comput. Chem. **3**, 317 (1982).
13. R.F.W. Bader and P.M. Beddall. J. Chem. Phys. **56**, 3320 (1972).
14. C. Nellin, B.O. Roos, A.J. Sadlej, and P.E.M. Siegbahn. J. Chem. Phys. **77**, 3607 (1982).
15. R.M. Glover and F. Weinhold. J. Chem. Phys. **65**, 4913 (1976).
16. P.W. Fowler and P.A. Madden. Phys. Rev. B, **29**, 1035 (1984).
17. R.E. Watson. Phys. Rev. **111**, 1108 (1958).
18. K.E. Laidig and R.F.W. Bader. J. Chem. Phys. **93**, 7213 (1990).
19. K.B. Wiberg and C. Breneman. J. Am. Chem. Soc. **112**, 8765 (1990).
20. R.G. Pearson. J. Chem. Educ. **64**, 561 (1987).